Cyanosphere Dynamic During Dolichospermum Bloom

Maxime Fuster, Thomas Ruiz, Amélie Lamarque, Marianne Coulon, Benjamin Legrand, Marion Sabart, Delphine Latour, Clarisse Mallet

Microbial Ecology (2024) 87:3
https://doi.org/10.1007/s00248-023-02317-4

RESEARCH

Cyanosphere Dynamic During *Dolichospermum* Bloom: Potential Roles in Cyanobacterial Proliferation

Maxime Fuster[1] · Thomas Ruiz[1] · Amélie Lamarque[1] · Marianne Coulon[1] · Benjamin Legrand[2] · Marion Sabart[1] · Delphine Latour[1] · Clarisse Mallet[1]

Received: 30 August 2023 / Accepted: 24 October 2023

Abstract
Under the effect of global change, management of cyanobacterial proliferation becomes increasingly pressing. Given the importance of interactions within microbial communities in aquatic ecosystems, a handful of studies explored the potential relations between cyanobacteria and their associated bacterial community (i.e., cyanosphere). Yet, most of them specifically focused on the ubiquitous cyanobacteria *Microcystis*, overlooking other genera. Here, based on 16s rDNA metabarcoding analysis, we confirmed the presence of cyanosphere representing up to 30% of the total bacterial community diversity, during bloom episode of another preponderant cyanobacterial genus, *Dolichospermum*. Moreover, we highlighted a temporal dynamic of this cyanosphere. A sPLS-DA model permits to discriminate three important dates and 220 OTUs. With their affiliations, we were able to show how these variations potentially imply a turnover in ecological functions depending on bloom phases. Although more studies are necessary to quantify the impacts of these variations, we argue that cyanosphere can have an important, yet underestimated, role in the modulation of cyanobacterial blooms.

Keywords Cyanobacterial bloom · Cyanosphere · Temporal dynamics · *Dolichospermum* · Ecological function

Introduction

Cyanobacterial proliferations constitute a major ecological concern in freshwater ecosystems worldwide. Under the effects of climate change and anthropogenic eutrophication, the intensity and frequency of such phenomena are expected to increase in the future [1–4]. The large-scale consequences of these ecological issues raised high scientific and public attention over the last decades, and the consequences of cyanobacterial blooms' toxicity for drinking water and recreational activities have been extensively studied as they may threaten human health [3]. Nonetheless, proliferations of toxic cyanobacteria constraint ecosystem structure and functions by impairing energy transfers along food chains [5, 6] or reducing water oxygenation [7], and subsequently jeopardize the ecosystemic services provided by aquatic environments [8–10]. In this context, predictions and management of cyanobacterial blooms, to mitigate their deleterious consequences on freshwater ecosystems and human populations, appear as a timely ecological task.

A promising, yet understudied, approach may focus on "cyanosphere," defined as microbial communities present in the narrow zone adjacent to cyanobacterial cells [11, 12]. The phycosphere, in general, exhibits high microbial diversity and abundance [13, 14] and may interact positively or negatively with adjacent phytoplanktonic cells [14–17]. For example, reciprocal exchanges of resources (e.g., nutrients, vitamins) may constitute driving factors mediating phytoplankton development [17, 18]. The importance of these interactions at the level of phytoplankton highlighted the necessity to question the role of such drivers for cyanobacterial proliferations specifically. Yet, the case of cyanosphere remains under-investigated [11, 12] and mainly assessed during *Microcystis* proliferations [19–22], thus complicating the generalization of the conclusions at the ecosystem scale. Nonetheless, cyanosphere may have important roles in modulating cyanobacterial communities as a whole [12, 23, 24]. The comprehension of these interactions could, *in fine*,

Maxime Fuster and Thomas Ruiz contributed equally to this work.

✉ Maxime Fuster
maxime.fuster@uca.fr

[1] Université Clermont Auvergne, CNRS, LMGE, F-63000 Clermont-Ferrand, France

[2] ATHOS Environnement, F-63000 Clermont-Ferrand, France

Published online: 27 November 2023

bring new insights in understanding and predicting cyanobacterial proliferation in aquatic environments.

Here, we explored the composition and specificity of the cyanosphere at different periods of a bloom dominated by the cyanobacterial genus *Dolichospermum*, which is known to induce severe cyanobacterial proliferation and may outperform *Microcystis*, given its ability to fix atmospheric nitrogen. Moreover, by integrating a temporal aspect, we aim at exploring the dynamics of cyanosphere along the cyanobacterial proliferation. Based on previously known roles of these communities, we highlight shifts in major ecological functions at different stages of bloom, suggesting potential roles of the cyanosphere on cyanobacterial development and performances.

Methods

Study Site and Sampling

Lake Aydat is an eutrophic lake located in the French Massif Central (45°39′53″N; 2°59′02″E ; 837 m altitude; 65 ha surface area; maximum depth: 15 m), with frequent autumnal blooms of cyanobacteria dominated by *Dolichospermum macrospora* [25–27]. During a period of 2 months ranging from August 24 to November 02, 2016, water was regularly sampled to follow cyanobacterial population dynamics (see details below) (Fig. 1). During this period, 6 different days during the bloom (14th and 21st of September; 12th, 19th, and 26th of October; and 2nd of November) were chosen to define bacterial communities by sequencing (Fig. 1). Water (0–3 m) was collected with integrative sampling pipe and immediately transported to the laboratory and stored at 4 °C until treatment (i.e., filtration and fixation). For each sample, raw samples were prefiltered on a 25 µm nylon filter to remove zooplankton. Then, microbial communities were collected with two successive filtrations: firstly, these filtrates were filtered on 8 µm (Millipore) polycarbonate filters (until saturation, pressure < 25 kPa) to obtain filamentous cyanobacteria and their attached bacterial communities (i.e., labeled attached fraction). Secondly, filtrates were filtered on 0.2 µm (Millipore) polycarbonate filters (until saturation, pressure < 25 kPa) to obtain free bacterial communities. All filtrations were realized in triplicate and stored at −20 °C until DNA extraction.

Bloom Characterization

The estimation of the total biomass of phytoplankton was inferred from in situ measurements of chlorophyll *a* using a submersible spectrofluorometric probe (BBE FluoroProbe, Moldaenke GmbH, DE). Determination of taxonomic composition and cell concentration of cyanobacteria were realized using 150 ml of water fixed by adding 10 ml of Lugol's iodine stock solution (Sigma-Aldrich, MA, USA) and stored in the dark at 4 °C. The counting process was carried out under an inverted microscope following the European Standard NF15204 [28], carried out by a specialized institute (ATHOS environment, Clermont-Ferrand, France) (Table s1). The cyanobacterial bloom was determined based on microscopic counts only as chlorophyll *a* was not sufficient to discriminate phytoplanktonic algae

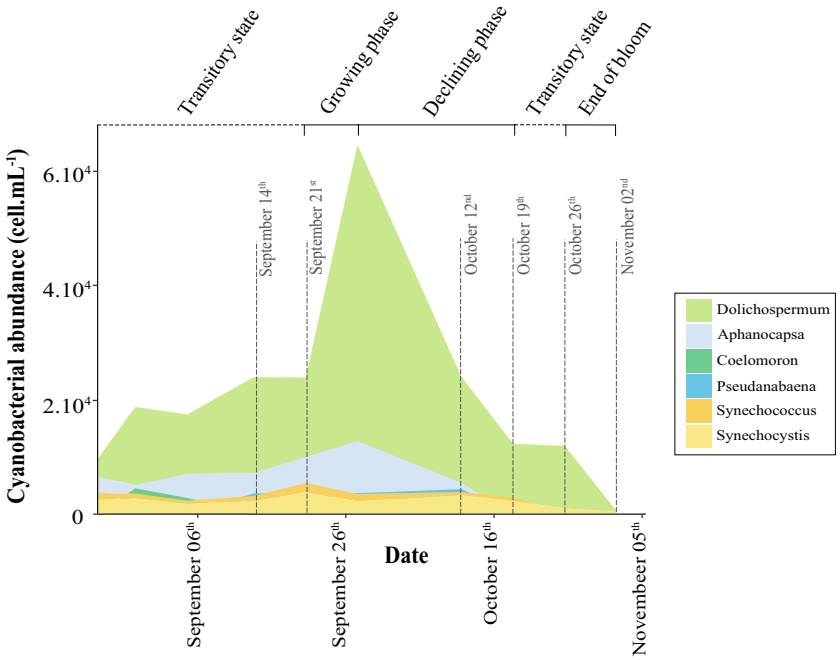

Fig. 1 Cyanobacterial abundance from August to November. Filtered and sequenced samples are represented by dashed lines. Different *genus* of cyanobacteria are represented by different colors. Bloom can be separated into three distinct phases: growing phase, declining phase, and end of bloom, interspersed with transitory states. *Dolichospermum* is the most abundant *genus* in any period, representing at least 80% of total abundance

from cyanobacteria. In accordance with values from the World Health Organization, we defined the bloom period when cyanobacterial cell exceeds 20,000 cells.mL^{-1}. Within the bloom, we defined the daily growth rate of cyanobacteria in percent of the total cyanobacterial population. When the growth exceeds 20% per day, it has been considered as a growing phase; when the decline is faster than 20% per day, it has been considered as declining phase.

Diversity of Microbial Communities

Nucleic Acid Extractions and Amplifications

All the filters were covered with a lysing buffer (lysozyme 2 mg.mL^{-1}, SDS 0.5%, Proteinase K 100 µg.mL^{-1}, and RNase A 8.33 µg.mL^{-1} in TE buffer pH 8) at 37 °C for 90 min. A CTAB 10%/NaCl 5 M solution was added, and the samples were incubated at 65 °C for 10 min. The nucleic acids were extracted with phenol–chloroform-isoamyl alcohol (25:24:1) followed by centrifugation (20 mn, 14,000g, 4 °C); the aqueous phase containing the nucleic acids was recovered and purified by adding chloroform-isoamyl alcohol (24:1) and centrifuged (30 mn, 14,000g, 4 °C). The nucleic acids were precipitated with cold isopropyl alcohol (0.6 V/V) during at least 1 h at −80 °C. After defrosting and centrifugation (20 mn, 14,000g, 4 °C), the DNA pellet was rinsed with ethanol (70%), centrifuged (30 mn, 14,000g, 4 °C), dried, and dissolved in 50 µL molecular grade water [29]. DNA quality and concentration were checked respectively with agarose gel and spectrophotometer NanoDrop™ (Thermo Fischer Scientific, MA, USA). To identify communities, the V4–V5 region of the bacterial small subunit rDNA was amplified using the universal bacteria 515F and 928R primers with Illumina Miseq adaptators [30] (Tab s2). PCR was performed in a total volume of 50 µL containing 1 X final reaction buffer, 2 mM $MgCl_2$, 0.2 mM dNTP, 100 µg mL^{-1} BSA, 0.2 µM of each primer, 0.025 U µL^{-1} PROMEGA GoTaq HotsStart G2 (Promega, Madison, USA), and 30 ng of DNA. The PCR program is detailed in the supplemental (Tab s2). PCR products were quantified with a Picogreen™ kit before being sent to the Genotoul platform (Toulouse, France) in a MySeq platform using a Reagent Kit v2 (2 × 250) (Illumina).

Amplicon Analysis and Taxonomic Affiliation

Bacterial sequencing data were analyzed through the FROGs pipeline [31]. Briefly, sequence reads were assembled with Vsearch [32] excluding reads < 200 bp, with ambiguous calls (N) or having mismatch in the forward/reverse primer. Demultiplexed amplicons were clustered into OTUs using Swarm [33] with distance (d) = 1. OTU sequences were compared against the SILVA_132_16s database. To avoid biases in our analysis, OTUs affiliated to cyanobacteria were removed.

Data Analysis

All the statistical analyses were performed using R software (v.4.1.3) [34]. Diversity indices were calculated on samples with phyloseq package for all indexes [35]. Differences in the diversity indices were determined by the Wilcoxon test. The average and standard deviations of these indices were then calculated for each fraction. The Venn diagram was constructed using the "MicrobiotaProcess" and "VennDiagram" packages [36, 37]. A Principal Coordinate Analysis (PCoA) based on the Bray-Curtis dissimilarity matrix using the "phyloseq" package was performed to explore (di)similarity in the structure of communities, function of fraction, and time. A Sparse Partial Least Squares-Discriminant Analysis (sPLS-DA) model using the "mixOmics" package was used to determine the discriminating dates and OTUs in our attached fraction [38]. OTUs affiliation and representation were performed using "phyloseq" and "ggplot2" packages [39]. Differences in the relative abundances between dates were determined by the χ^2 test. A literature review was performed by combining results from PubMed and Google Scholar. The role of the cyanosphere was reviewed individually for each species and/or at the level of the genus when species information was unavailable. For each species/genus, we searched the species/genus name followed by "function," "metabolism," and "ecological features.

Results

Characterization of Cyanobacterial Bloom Dynamics

Based on cyanobacterial counts, we characterized the bloom's dynamics over approximately 2 months (Fig. 1). Three major phases could be highlighted. Firstly, a phase characterized by rapid cyanobacterial growth, with a peak concentration of 6.43 × 10^4 cells/mL, was reached on September 28th (Fig. 1). Between September 28th and October 19th, a rapid decline in the cyanobacterial population constituted the second phase of the bloom (Fig. 1). The end of the bloom constituted the third phase (Fig. 1), with the lowest cyanobacterial abundance reported (3.82 × 10^2 cells/mL) on November 2nd. The cyanobacterial community, composed of six different genera, was largely dominated by *Dolichospermum*, representing more than 80% of the total cell abundance during the entire period of the study.

Bacterial Diversity and Structure Comparison Between Cyanosphere and Free Fraction

After cleaning, a total of 431,058 reads distributed across 2429 OTUs were obtained from 16S rRNA gene sequencing. On average, 11,974 reads were obtained per sample. Bacterial α-diversity varied statistically among samples ($V = 171$, $p < .001$, Wilcoxon test): the highest diversity was recorded in the attached fraction, regardless of the diversity index used (Fig. 2A). More specifically, 687 OTUs (28% of the total OTUs) were specific to the attached fraction, while only 219 OTUs (9% of the total OTUs) were present in the free fraction (Fig. 2B). PCoA was performed to explore (dis)similarity between the attached and free fractions based on this diversity (Fig. 3). The first two axes account for 68.7% of the total variance (Fig. 3). The first axis strongly and significantly separates our different fractions into two distinct clusters (Fig. 3). The second axis clearly separates our samples according to the dates of sampling in chronological order, highlighting a difference in community depending on the bloom's period, in addition to differences reported for fractions (Fig. 3). Among these fractions, we therefore highlight differences between the free fraction and the cyanosphere.

Temporal Dynamics of Structure and Functions of Cyanosphere

A multivariate model (sPLS-DA) was performed to enhance sample discrimination in the attached fraction and identify discriminating OTUs throughout the bloom (Fig. 4, Fig. S1). Three sampling dates are highly significantly discriminated in the cyanosphere: 21st September 12th October, and 02nd November, respectively, corresponding to the beginning of the growing phase, declining phase, and end of the bloom (Fig. 4). The three other dates, corresponding to transitory phases, are close and did not show a significant difference between them (Fig. 4). A Clustered Image Map (CIM) of specific OTUs of the attached fraction, based on the

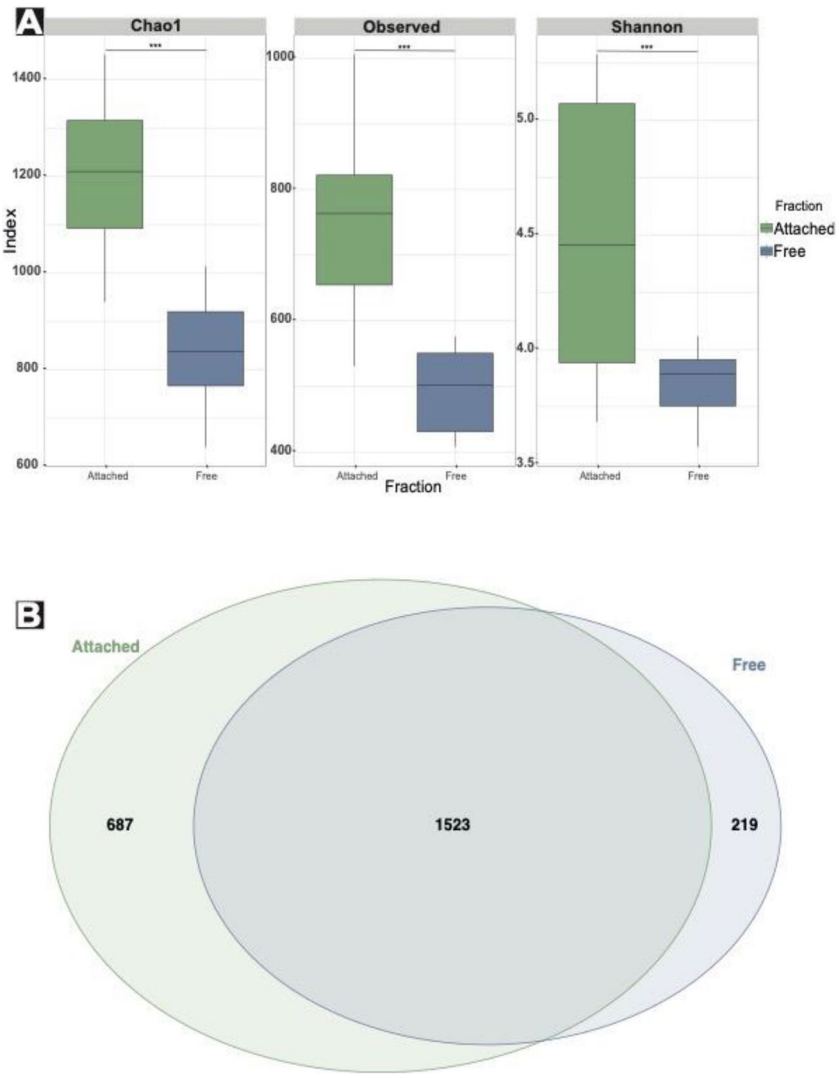

Fig. 2 Diversity index function of observed fraction (**A**) and Venn diagram representing the number of OTUs specific to each fraction or in common (**B**), all dates combined. Each fraction was represented by different colors. *** = $p < .001$, V = 171, Wilcoxon test

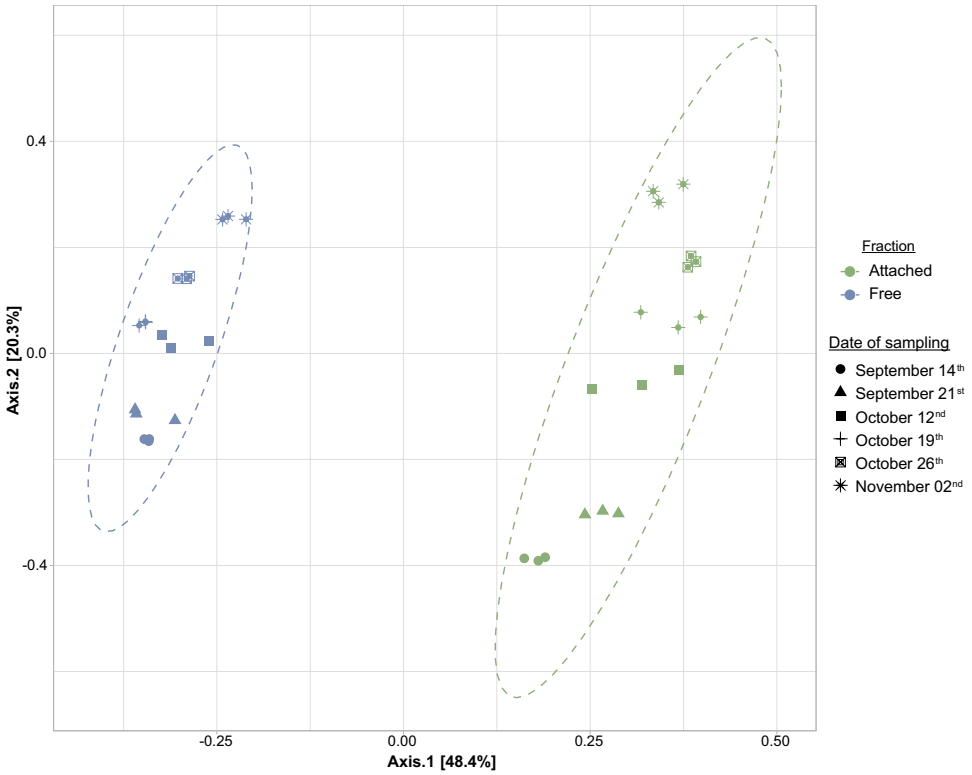

Fig. 3 Principal coordinates analysis plot on different bacterial fractions and sampling dates. Results of PCoA showing the first two principal coordinates that, combined, explain 68.7% of observed variation. Shapes on the figure legend correspond to the different sampling dates. Colors correspond to the two different fractions. Ellipses show 95% CI

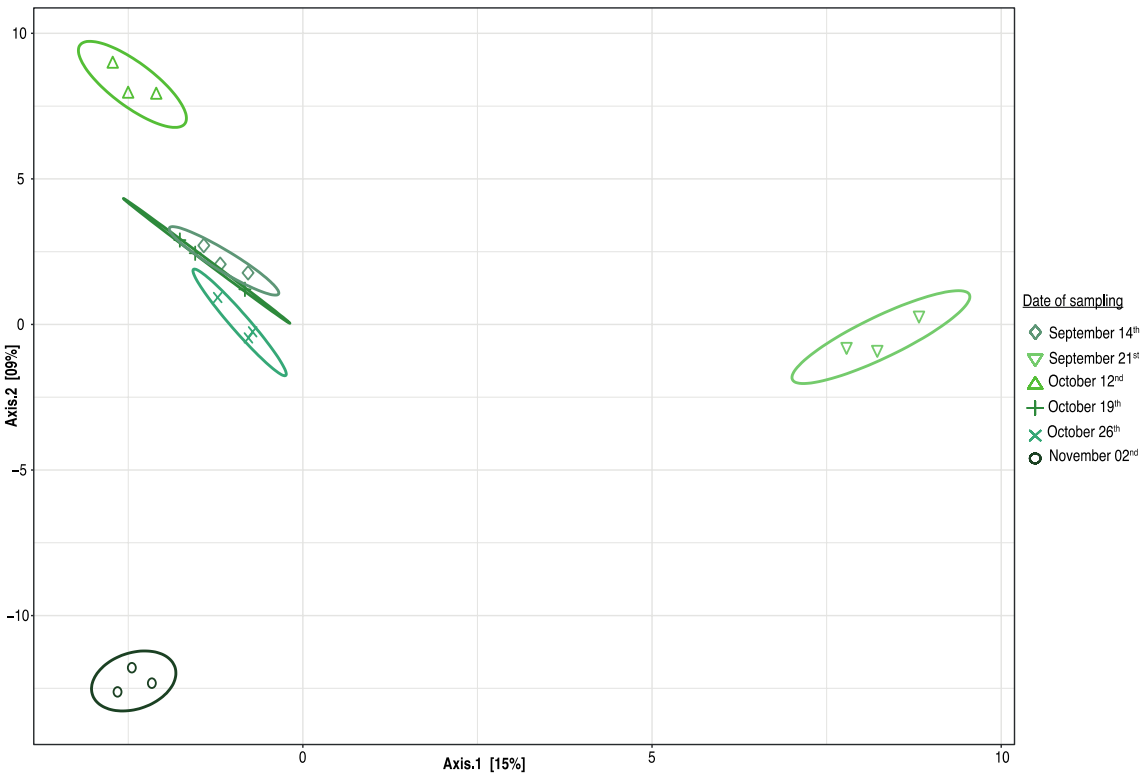

Fig. 4 Sample plots after a basic sPLS-DA model operated on attached fraction. sPLS-DA model makes it possible to significantly and distinctly separate three distinctive dates during the bloom period. Ellipses show 95% CI. Three grouped dates (September 14th, October 19th and 26th) all correspond to transitory state of the bloom. September 21st match with the beginning of the growing phase, October 12th with the declining phase and November 02nd with the end of bloom

sPLS-DA, points out the results reported above, highlighting different discriminant OTUs across the three important dates (Fig. S1).

Concerning our three discriminative dates, 220 discriminating OTUs determined by our sPLS-DA model are distributed across 65 different orders from 14 different phyla (Fig. 5, Table S3). Among these phyla, three are predominant: Actinobacteria, Bacteroidetes, and Proteobacteria (Fig. 5). Regarding orders, significant variations in relative abundance were recorded between the three discriminant dates (χ^2 test, $DF = 100$, $p < .001$) (Fig. 5). As shown in Fig. 5, the beginning of the growing phase was dominated by Chitinophagales, Rhodobacterales, and Sphingomonadales. Pirellulales and Rhizobiales were abundant during the declining phase of the bloom, while Flavobacteriales,

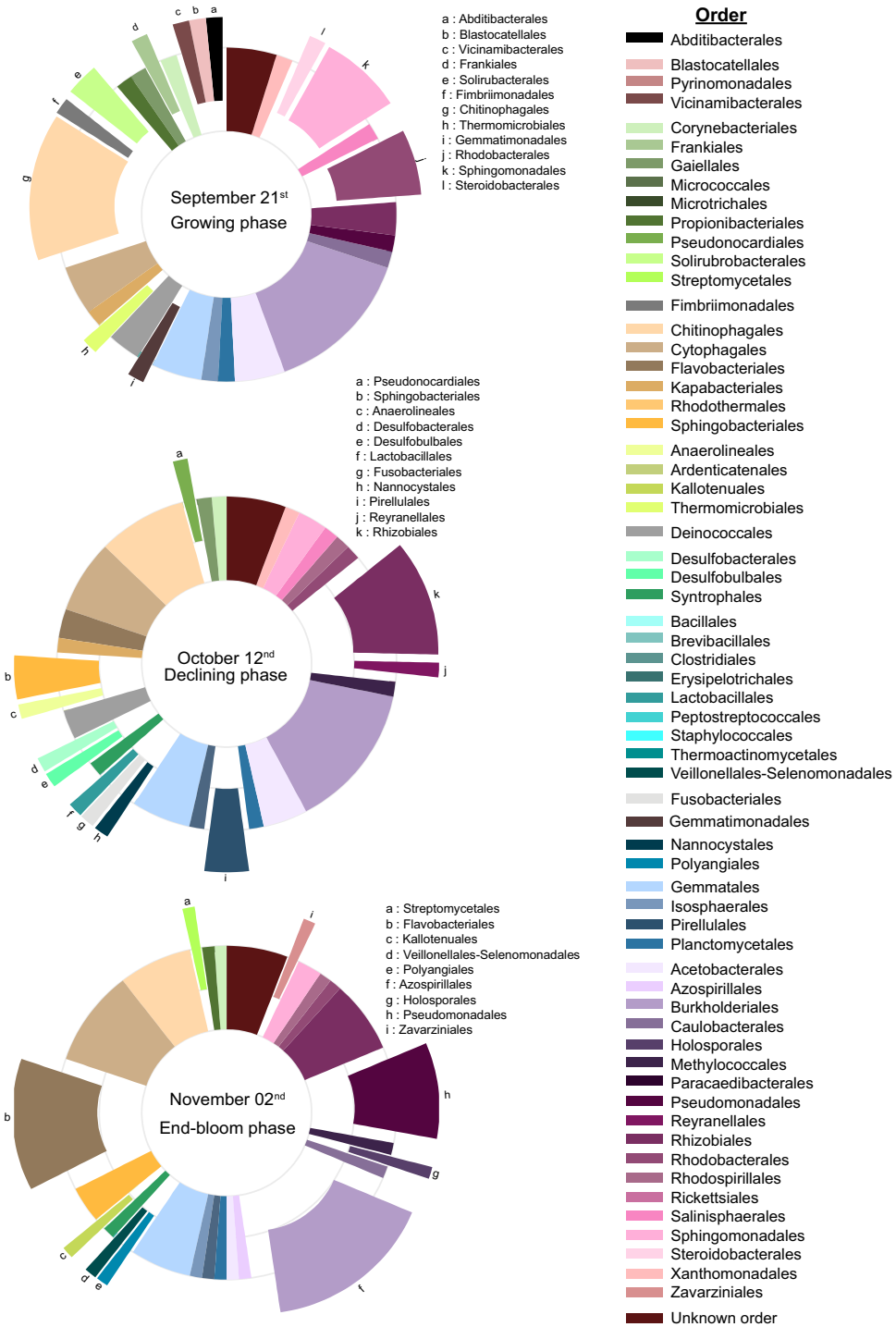

Fig. 5 Taxonomic affiliation of bacterial OTUs belonging to the attached fraction at three discriminant dates of the bloom. Affiliations are made at the order level. The orders are classified by their phyla to which they belong. The differenced orders numbered by letters represent significant relative abundance variations for each time (χ^2 test, $DF = 100$, $p < .001$)

Azospirillales, and Pseudomonales dominated at the end of the bloom.

For each of the 220 OTUs, we defined their relevant biological features based on a literature analysis (a literature analysis was performed for each OTU individually at the finest possible taxonomic level, from species to family). These features were sorted under 7 main ecological functions (see Fig. 6 for details) exhibiting significant variations at different bloom periods (χ^2 test, $DF = 14$, $p < .001$) (Fig. 6, Table S3). During the growing phase of the bloom, the degradation of toxicants (cyanotoxins, chemical pollutants, and heavy metals) was significantly more represented than in other bloom periods (Fig. 6, Table S3). The declining phase of the bloom is mainly characterized by important proportions of orders associated with biofilm formation (Fig. 6, Table S3). In addition, the declining phase also exhibits an increased number of other orders involved in various marginal functions (Fig. 6, Table S3). Production of algicidal compounds was statistically more represented at the end of the bloom than in the two previous phases (Fig. 6, Table S3). Finally, functions associated with organic matter cycles are dominant during all stages of the bloom, despite specific changes regarding the preferred compounds of this organic matter (C, N, or P). More specifically, N is dominant in the declining phase, and C is dominant at the end of the bloom (Fig. 6, Table S3).

Discussion

This study followed the composition of freshwater bacterial communities during 7 weeks of an autumnal cyanobacterial bloom dominated by *Dolichospermum* (Fig. 1). We showed the presence of a specific bacterial community associated to cyanobacteria, significantly differing from the free bacterial community (Figs. 2A and 3). Here, the bacterial diversity of the attached fraction can exceed the one of the free communities (Fig. 2), representing almost 30% of the total bacterial diversity versus only 9% for the free community. The last 61% being common to both attached and free communities. This result supports the concept of cyanosphere (i.e., bacterial communities associated to cyanobacteria) mainly drawn from studies focusing on *Microcystis* bloom [12, 19–22]. While the composition of this cyanosphere may vary depending on the dominant cyanobacterial species constituting the bloom [11], our results tend to nuance this conclusion. We showed that *Dolichospermum* and *Microcystis* cyanospheres may present some similarities at the phylum level, with Proteobacteria and Bacteroïdetes being reported as dominant phyla in both [20, 21] (Fig. 5). In contrast, Liu et al. (2018) [40] showed a predominance of Actinobacteria during *Microcystis* bloom, a conclusion differing from the one of Jankowiak and Gobler (2020, 2022) [20, 21]. This apparent contradiction suggests that the composition of cyanosphere may be influenced by the dominant cyanobacteria [11], but probably also by other environmental factors, which remains to be defined.

Moreover, beyond the observed cyanosphere variability between different cyanobacterial blooms from the same and/or different cyanobacterial genera, our study constitutes one of the first evidence that cyanosphere composition exhibits temporal variation during a same bloom event. Three specific dates appeared significantly discriminant in our model. These dates match critical phases of bloom dynamics: (i) the growing phase, (ii) the declining phase, and (iii) the end of the bloom. The three other sequenced samples were not discriminative and matched with transitory states present between the critical phases described above. This clear temporal variation highlights the dynamic aspect of cyanosphere composition depending on the bloom's phases. Such

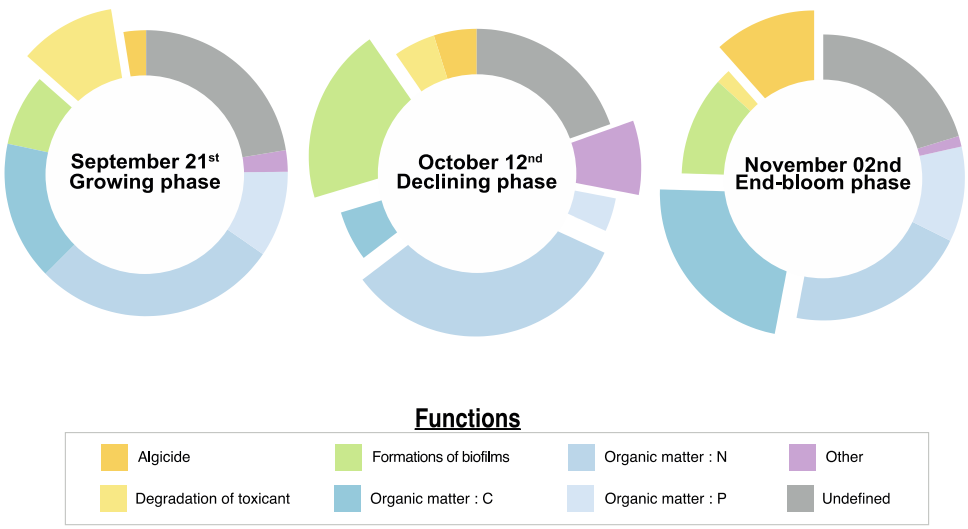

Fig. 6 Function affiliation of bacterial OTUs belonging to attached fraction at three discriminant dates of bloom. Affiliation of major ecological functions based on literature data (see Supp. Tab. 2 for details). The differenced functions represent the significant relative abundance variations for each time (χ^2 test, $DF = 14$, $p < .001$

variation of cyanosphere composition may lead to shifts in its ecological functions.

During the growing phase, ecological functions supported by this cyanosphere were mainly generalist. Among all functions, the only one being significantly more represented was the degradation of toxicant, such as antibacterial compounds (e.g., Solirubacterales) and/or cyanotoxins (e.g., Sphingomonadales) (Fig. 5, Fig. S1, Tab S3) [41], possibly affecting directly and indirectly the development of *Dolichospermum* and their associate cyanosphere.

After its peak, the bloom enters in a declining phase characterized by an important proportion of OTUs associated to the formation of biofilm (e.g., Rhizobiales order) (Fig. 5, Fig. S1, Tab S3). Biofilm formation, based on the production of EPS (ExtracellularPolymericSubstants), could be an important factor to regulate the cyanobacterial bloom. The formation of biofilm can control the development of cyanobacteria, particularly the *Microcystis* and *Dolichospermum* genera, limiting their growth by blocking their photosynthetic capacity either directly by secreting substances disrupting photosystems or indirectly by reducing incident light [42, 43]. This phase is also characterized by a significant proportion of OTUs involved in the nitrogen cycle (e.g., Rhizobiales, Pirellulales) [44–46] (Fig. 5, Fig. S1, Tab S3), probably resulting from the increased release of organic matter associated with cyanobacterial senescence. In addition, it has also been shown that Rhizobiales have the ability to directly lyse *Microcystis* [47], here potentially playing a role in bloom decline.

At the end of the bloom, the most notable function was the production of algicidal compounds by a highly prevalent order in our dataset (i.e., Flavobacteriales) [48] (Fig. 5, Fig. S1, Tab S3). The ability of Flavobacteriales to lyse cyanobacteria will lead to the active degradation of senescent cells into POM (particulate organic matter) and/or DOM (dissolved organic matter), subsequently releasing bio-available nutrients and/or oligo-elements in freshwater ecosystems after periods of blooms. This process, known in oceanic environments [49, 50], will support the microbial loop and subsequently the functioning of the entire ecosystem. The increase of POM/DOM in the environment may induce an increase of orders involved in the carbon cycle, which is the second most significant function reported in this phase of the bloom.

At a wider scale, phytoplanktonic blooms represent an important turnover of organic matter in aquatic ecosystems [48]. Given its direct and indirect roles, the cyanosphere may constitute one important, yet underestimated, regulator of cyanobacterial blooms. Although our results constitute an important step toward the understanding of cyanosphere role, our conclusions are based on the 16s rDNA metabarcoding analysis, only exploring the potential ecological functions of our known OTUs. For technical reasons, we were not able to integrate data at the peak of the bloom, but it could be interesting to integrate such data to study potential community shifts. Further studies are necessary to assess the level of expression of these potential functions, to fully anticipate the impacts of the cyanosphere on cyanobacterial proliferation and, at a wider scale, aquatic environments.

In conclusion, our study confirms the presence of a specific cyanosphere associated with *Dolichospermum* and, for the first time to our knowledge, highlights its temporal dynamics during the bloom. Furthermore, we showed that significant variations in community structure potentially led to shifts in associated ecological features. Cyanobacteria, and particularly *Dolichospermum*, are known to produce high cell density during the bloom (more than other phytoplanktonic species), inducing a wide diversity of cyanosphere, as we observed in this study. In this context, these bacterial communities may play a key role, not only in controlling the cyanobacterial microhabitat but also in modulating matter and energy fluxes at the ecosystem level.

Supplementary Information The online version contains supplementary material available at https://doi.org/10.1007/s00248-023-02317-4.

Acknowledgements We are grateful to the genotoul bioinformatics platform Toulouse Midi-Pyrenees for providing sequencing and the pre-treatment of sequences.

Author Contributions A.L, M.C, M.S, and B.L collected and processed samples. M.F and T.R processed data analysis and prepared figures. M.F, T.R, D.L, and C.M wrote the main manuscript text. All authors reviewed the manuscript.

Funding This work was supported by the FEDER Loire – Plan Loire grandeur nature and the "Etablissement Public Loire."

Data Availability The dataset generated during and/or analyzed during the current study is available in the Bioproject repository, ID PRJNA996867. R script and supplemental table in .csv file are available on GitHub: https://github.com/MxFtr/Diversitox.

Declarations

Competing Interests The authors declare no competing interests.

References

1. Sukenik A, Quesada A, Salmaso N (2015) Global expansion of toxic and non-toxic cyanobacteria: effect on ecosystem functioning. Biodivers Conserv 24:889–908. https://doi.org/10.1007/s10531-015-0905-9
2. Legrand B, Lamarque A, Sabart M, Latour D (2017) Benthic archives reveal recurrence and dominance of toxigenic cyanobacteria in a eutrophic lake over the last 220 years. Toxins 9:271. https://doi.org/10.3390/toxins9090271
3. Huisman J, Codd GA, Paerl HW et al (2018) Cyanobacterial blooms. Nat Rev Microbiol 16:471–483. https://doi.org/10.1038/s41579-018-0040-1

4. Smucker NJ, Beaulieu JJ, Nietch CT, Young JL (2021) Increasingly severe cyanobacterial blooms and deep water hypoxia coincide with warming water temperatures in reservoirs. Glob Change Biol 27:2507–2519. https://doi.org/10.1111/gcb.15618
5. Ruiz T, Koussoroplis A, Danger M et al (2021) Quantifying the energetic cost of food quality constraints on resting metabolism to integrate nutritional and metabolic ecology. Ecology Letters 24:2339–2349. https://doi.org/10.1111/ele.13855
6. Ruiz T, Koussoroplis A-M, Latour D, Bec A (2022) The energetic cost of facing cyanotoxins: a case study on Daphnia magna. Aquat Ecol. https://doi.org/10.1007/s10452-022-09990-6
7. Paerl HW, Huisman J (2009) Climate change: a catalyst for global expansion of harmful cyanobacterial blooms. Environ Microbiol Rep 1:27–37. https://doi.org/10.1111/j.1758-2229.2008.00004.x
8. Tillmanns AR, Wilson AE, Pick FR, Sarnelle O (2008) Meta-analysis of cyanobacterial effects on zooplankton population growth rate: species-specific responses. fal 171:285–295. https://doi.org/10.1127/1863-9135/2008/0171-0285
9. Drobac D, Tokodi N, Lujić J et al (2016) Corrigendum to "Cyanobacteria and cyanotoxins in fishponds and their effects on fish tissue" [Harmful Algae 55 (2016) 66–76]. Harmful Algae 55:296. https://doi.org/10.1016/j.hal.2016.03.018
10. Edmondson WT, Litt AH (1982) *Daphnia* in Lake Washington1: Daphnia *in Lake Washington*. Limnol Oceanogr 27:272–293. https://doi.org/10.4319/lo.1982.27.2.0272
11. Louati I, Pascault N, Debroas D et al (2015) Structural diversity of bacterial communities associated with bloom-forming freshwater cyanobacteria differs according to the cyanobacterial genus. PLoS ONE 10:e0140614. https://doi.org/10.1371/journal.pone.0140614
12. Cai H, Jiang H, Krumholz LR, Yang Z (2014) Bacterial community composition of size-fractioned aggregates within the phycosphere of cyanobacterial blooms in a eutrophic freshwater lake. PLoS ONE 9:e102879. https://doi.org/10.1371/journal.pone.0102879
13. Azam F, Malfatti F (2007) Microbial structuring of marine ecosystems. Nat Rev Microbiol 5:782–791. https://doi.org/10.1038/nrmicro1747
14. Amin SA, Hmelo LR, van Tol HM et al (2015) Interaction and signalling between a cosmopolitan phytoplankton and associated bacteria. Nature 522:98–101. https://doi.org/10.1038/nature14488
15. Fouilland E, Tolosa I, Bonnet D et al (2014) Bacterial carbon dependence on freshly produced phytoplankton exudates under different nutrient availability and grazing pressure conditions in coastal marine waters. FEMS Microbiol Ecol 87:757–769. https://doi.org/10.1111/1574-6941.12262
16. Buchan A, LeCleir GR, Gulvik CA, González JM (2014) Master recyclers: features and functions of bacteria associated with phytoplankton blooms. Nat Rev Microbiol 12:686–698. https://doi.org/10.1038/nrmicro3326
17. Amin SA, Parker MS, Armbrust EV (2012) Interactions between diatoms and bacteria. Microbiol Mol Biol Rev 76:667–684. https://doi.org/10.1128/MMBR.00007-12
18. Seymour JR, Amin SA, Raina J-B, Stocker R (2017) Zooming in on the phycosphere: the ecological interface for phytoplankton–bacteria relationships. Nat Microbiol 2:17065. https://doi.org/10.1038/nmicrobiol.2017.65
19. Chen S, Yan M, Huang T et al (2020) Disentangling the drivers of Microcystis decomposition: metabolic profile and co-occurrence of bacterial community. Sci Total Environ 739:140062. https://doi.org/10.1016/j.scitotenv.2020.140062
20. Jankowiak JG, Gobler CJ (2020) The composition and function of microbiomes within microcystis colonies are significantly different than native bacterial assemblages in two north American lakes. Front Microbiol 11:1016. https://doi.org/10.3389/fmicb.2020.01016
21. Gobler CJ, Jankowiak JG (2022) Dynamic responses of endosymbiotic microbial communities within microcystis colonies in north American lakes to altered nitrogen, phosphorus, and temperature levels. Front Microbiol 12:781500. https://doi.org/10.3389/fmicb.2021.781500
22. Mankiewicz-Boczek J, Font-Nájera A (2022) Temporal and functional interrelationships between bacterioplankton communities and the development of a toxigenic Microcystis bloom in a lowland European reservoir. Sci Rep 12:19332. https://doi.org/10.1038/s41598-022-23671-2
23. Pascault N, Rué O, Loux V et al (2021) Insights into the cyanosphere: capturing the respective metabolisms of cyanobacteria and chemotrophic bacteria in natural conditions? Environ Microbiol Rep 13:364–374. https://doi.org/10.1111/1758-2229.12944
24. Zhang Q, Zhang Z, Lu T et al (2020) Cyanobacterial blooms contribute to the diversity of antibiotic-resistance genes in aquatic ecosystems. Commun Biol 3:737. https://doi.org/10.1038/s42003-020-01468-1
25. Gerphagnon M, Latour D, Colombet J, Sime-Ngando T (2013) Fungal parasitism: life cycle, dynamics and impact on cyanobacterial blooms. PLoS ONE 8:e60894. https://doi.org/10.1371/journal.pone.0060894
26. Sabart M, Crenn K, Perrière F et al (2015) Co-occurrence of microcystin and anatoxin-a in the freshwater lake Aydat (France): analytical and molecular approaches during a three-year survey. Harmful Algae 48:12–20. https://doi.org/10.1016/j.hal.2015.06.007
27. Legrand B, Lamarque A, Sabart M, Latour D (2016) Characterization of akinetes from cyanobacterial strains and lake sediment: a study of their resistance and toxic potential. Harmful Algae 59:42–50. https://doi.org/10.1016/j.hal.2016.09.003
28. AFNOR (2006) Qualité de l'eau - Norme guide pour le dénombrement du phytoplancton par microscopie inversée (méthode Utermöhl). NF EN 15204, p 41. https://www.boutique.afnor.org/fr-fr/norme/nf-en-15204/qualitede-leau-norme-guide-pour-le-denombrement-du-phytoplancton-parmicro/fa136619/814#AreasStoreProductsSummaryView
29. Zhou J, Bruns MA, Tiedje JM (1996) DNA recovery from soils of diverse composition. Appl Environ Microbiol 62:316–322. https://doi.org/10.1128/aem.62.2.316-322.1996
30. Wang Y, Qian P-Y (2009) Conservative fragments in bacterial 16S rRNA genes and primer design for 16S ribosomal DNA amplicons in metagenomic studies. PLOS ONE 4:e7401. https://doi.org/10.1371/journal.pone.0007401
31. Escudié F, Auer L, Bernard M et al (2018) FROGS: find, rapidly, OTUs with galaxy solution. Bioinformatics 34:1287–1294. https://doi.org/10.1093/bioinformatics/btx791
32. Kim M, Morrison M, Yu Z (2011) Evaluation of different partial 16S rRNA gene sequence regions for phylogenetic analysis of microbiomes. J Microbiol Methods 84:81–87. https://doi.org/10.1016/j.mimet.2010.10.020
33. Mahé F, Czech L, Stamatakis A et al (2022) Swarm v3: towards tera-scale amplicon clustering. Bioinformatics 38:267–269. https://doi.org/10.1093/bioinformatics/btab493
34. R Core Team (2021). R: A language and environment for statistical computing. R Foundation for Statistical Computing, Vienna, Austria. https://www.R-project.org/
35. McMurdie PJ, Holmes S (2013) phyloseq: An R package for reproducible interactive analysis and graphics of microbiome census data. PLoS ONE 8:e61217. https://doi.org/10.1371/journal.pone.0061217
36. Xu S, Zhan L, Tang W et al (2023) MicrobiotaProcess: a comprehensive R package for deep mining microbiome. Innovation 4:100388. https://doi.org/10.1016/j.xinn.2023.100388

37. Chen H, Boutros PC (2011) VennDiagram: a package for the generation of highly-customizable Venn and Euler diagrams in R. BMC Bioinform 12:35. https://doi.org/10.1186/1471-2105-12-35
38. Rohart F, Gautier B, Singh A, Lê Cao K-A (2017) mixOmics: an R package for 'omics feature selection and multiple data integration. PLoS Comput Biol 13:e1005752. https://doi.org/10.1371/journal.pcbi.1005752
39. Wickham H (2009) ggplot2: Elegant graphics for data analysis. Springer New York, New York, NY. https://doi.org/10.1007/978-0-387-98141-3
40. Liu M, Liu L, Chen H et al (2019) Community dynamics of free-living and particle-attached bacteria following a reservoir Microcystis bloom. Sci Total Environ 660:501–511. https://doi.org/10.1016/j.scitotenv.2018.12.414
41. KAR K, Lymperopoulou DS (2013) Cyanobacterial toxin degrading bacteria: who are they? BioMed Res Int 2013:1–12. https://doi.org/10.1155/2013/463894
42. Wu Y, Liu J, Yang L et al (2011) Allelopathic control of cyanobacterial blooms by periphyton biofilms: allelopathic control of cyanobacterial blooms. Environ Microbiol 13:604–615. https://doi.org/10.1111/j.1462-2920.2010.02363.x
43. Van Le V, Ko S-R, Kang M et al (2023) Periphyton reduces cyanobacterial blooms by promoting potentially cyanobactericidal bacteria. J Appl Phycol 35:1285–1299. https://doi.org/10.1007/s10811-023-02949-6
44. Dourado MN, Aparecida Camargo Neves A, Santos DS, Araújo WL (2015) Biotechnological and agronomic potential of endophytic pink-pigmented methylotrophic *Methylobacterium* spp. BioMed Res Int 2015:1–19. https://doi.org/10.1155/2015/909016
45. Wiegand S, Jogler M, Jogler C (2018) On the maverick Planctomycetes. FEMS Microbiol Rev 42:739–760. https://doi.org/10.1093/femsre/fuy029
46. Andrei A-Ş, Salcher MM, Mehrshad M et al (2019) Niche-directed evolution modulates genome architecture in freshwater Planctomycetes. ISME J 13:1056–1071. https://doi.org/10.1038/s41396-018-0332-5
47. Pal M, Purohit HJ, Qureshi A (2021) Genomic insight for algicidal activity in Rhizobium strain AQ_MP. Arch Microbiol 203:5193–5203. https://doi.org/10.1007/s00203-021-02496-z
48. Meyer N, Bigalke A, Kaulfuß A, Pohnert G (2017) Strategies and ecological roles of algicidal bacteria. FEMS Microbiol Rev 41:880–899. https://doi.org/10.1093/femsre/fux029
49. Mayali X, Azam F (2004) Algicidal bacteria in the sea and their impact on algal blooms1. J Eukaryotic Microbiology 51:139–144. https://doi.org/10.1111/j.1550-7408.2004.tb00538.x
50. Roy S, Chattopadhyay J (2007) The stability of ecosystems: a brief overview of the paradox of enrichment. J Biosci 32:421–428. https://doi.org/10.1007/s12038-007-0040-1